

# Field measurements of three-dimensional hydraulics in a step-pool channel

Andrew C. Wilcox <sup>\*</sup>, Ellen E. Wohl

*Department of Geosciences, Colorado State University, Fort Collins, CO 80523, USA*

Received 5 May 2005; received in revised form 13 February 2006; accepted 13 February 2006

Available online 5 July 2006

## Abstract

We investigated the effects of morphologic position and discharge on flow structure in a steep (0.10 m/m) mountain channel by collecting three-dimensional measurements of time-averaged and turbulent velocity components with a SonTek FlowTracker Handheld ADV (acoustic Doppler velocimeter) on a 30-m reach of a step-pool channel in the Colorado Rockies. Velocity profiles were measured at morphologic positions characteristic of steep channels (above steps, step lips, base of steps, pools, cascades, runs), and at five different discharges. A marked three-dimensionality of flow structure was documented in East St. Louis Creek. Velocities in the streamwise component were the largest contributors to overall velocity vector magnitudes; cross-stream and vertical components contributed averages of 20% and 15%, respectively, to overall vector magnitudes. Turbulence intensities were especially multi-dimensional, however, with large contributions to turbulent kinetic energy from the vertical component of velocity. Analysis of variance indicated that discharge and morphologic position significantly affected mean streamwise velocities, with substantially higher velocities upstream from steps than in pools. Discharge and morphology effects on cross-stream and vertical velocity components, however, were not significant. Discharge and morphologic position also significantly affected turbulence intensities for all flow components, with the greatest turbulence intensities occurring in pools and at high discharges. These results illustrate the strong discharge-dependence of hydraulics in step-pool channels, where relative submergence of bedforms changes rapidly with discharge, and the substantial spatial variation in hydraulics created by step-pool sequences.

© 2006 Elsevier B.V. All rights reserved.

*Keywords:* Velocity; Step-pool channel; Turbulence intensity; Acoustic Doppler velocimeter; FlowTracker

## 1. Introduction

Step-pool channels are an important class of mountain channels that are characterized by steep gradients (0.02–0.20 m/m) and repeating sequences of boulder, log, or bedrock steps and intervening pools

(Chin and Wohl, 2005). Hydraulics and morphology in step-pool channels are tightly coupled, with flow resistance resulting from the form drag of step-forming clasts and/or logs and from spill over steps into downstream pools (Curran and Wohl, 2003; MacFarlane and Wohl, 2003; Wilcox et al., 2006). Flow hydraulics in step-pool channels have been described in terms of a “tumbling” flow regime in which critical or supercritical flow over step crests plunges into downstream pools, where velocity abruptly decreases and hydraulic jumps and roller eddies generate

<sup>\*</sup> Corresponding author. Present address: U.S. Geological Survey, National Research Program, Geomorphology and Sediment Transport Laboratory, Golden, CO 80403, USA.

*E-mail address:* [awilcox@usgs.gov](mailto:awilcox@usgs.gov) (A.C. Wilcox).

substantial turbulence (Peterson and Mohanty, 1960; Wohl and Thompson, 2000).

Despite the apparently multi-dimensional character of flow structure created by step-pool sequences, hydraulics in step-pool channels have not been previously investigated in a three-dimensional framework. This is emblematic of a general lag in research on hydraulics in steep stream channels behind related work on lower-gradient channels. Recent work has nevertheless substantially advanced knowledge of physical processes in steep channels, including investigations of flow resistance dynamics (Lee and Ferguson, 2002; Yager et al., 2002; Curran and Wohl, 2003; MacFarlane and Wohl, 2003; Wilcox et al., 2006; Wilcox and Wohl, 2006); formative processes of step-pool sequences (Whittaker and Jaeggi, 1982; Abrahams et al., 1995); controls on step spacing and geometry (Grant et al., 1990; Wohl and Grodek, 1994; Chin, 1999; Chartrand and Whiting, 2000; Zimmerman and Church, 2001; Curran and Wilcock, 2005; Milzow et al., 2006); mathematical treatment of flow structure (Furbish, 1993; Furbish, 1998); pool scour and jet characteristics (Comiti, 2003; Comiti et al., 2005); hydraulic jumps (Valle and Pasternack, 2006); and the morphologic effects of woody debris (Jackson and Sturm, 2002; Faustini and Jones, 2003). Building on these studies with further work exploring the interactions between hydraulics and bedforms is critical to developing insight into sediment transport and formative processes in step-pool channels.

One field study of hydraulics in step-pool channels (Wohl and Thompson, 2000) described velocity fluctuations in a step-pool channel using measurements with a one-dimensional electromagnetic current meter at various discharges and positions with respect to bedform type. Velocity profiles suggested that sites in pools immediately downstream from bed steps are dominated by wake turbulence from mid-profile shear layers associated with roller eddies, whereas sites upstream from steps, at steps, and in runs are dominated by bed-generated turbulence (Wohl and Thompson, 2000). Wohl and Thompson (2000) suggest that higher energy dissipation results from the wake-generated turbulence and form drag of step-pool reaches compared to the bed-generated turbulence found in more uniform-gradient reaches such as runs. Wohl and Thompson also found that as discharge increases, the magnitude of velocity fluctuations increase, with the largest increases recorded downstream from steps.

In lower-gradient river systems, several workers have completed field studies of flow structure and characteristics of turbulence in a multi-dimensional framework.

These studies have investigated a range of processes in sand- and gravel-bed rivers, including for example the role of vortex shedding around roughness elements and development of separation zones as a mechanism of momentum exchange (Robert et al., 1992; Robert, 1993; Buffin-Belanger and Roy, 1998); reach-scale variability in velocity and turbulence (Lamarre and Roy, 2005; Legleiter et al., 2007); the size, scale, and dynamics of macro-turbulent flow structures (Roy et al., 2004); the effect of roughness transitions on turbulence intensities (Robert et al., 1996); the role of burst events in sand suspension (Lapointe, 1992); and analysis of three-dimensional velocities and/or turbulence at confluences (Sukhodolov and Rhoads, 2001) and associated with woody debris (Daniels and Rhoads, 2003).

This work has been facilitated by technological advances in instrumentation, including the development of current meters capable of field measurements of velocity and turbulence in a two- or three-dimensional framework (Lane et al., 1998; Walker and Roy, 2005). Application of acoustic Doppler methods for measuring three-dimensional velocity fields, including acoustic Doppler velocimeters (ADV) (e.g., Lane et al., 1998) and acoustic Doppler current profilers (ADCPs) (e.g., Kostaschuk et al., 2005), has become increasingly well established in low- and moderate-gradient river systems (see for example the list of ADV studies in Buffin-Belanger and Roy, 2005). Analogous data collection has not been previously performed in high-gradient stream channels, however, reflecting the challenges presented by complex topography and hydraulics in these systems. Flow that can be locally highly aerated and turbulent, coarse and heterogeneous bed substrates, and remote settings create unique challenges for any method of velocity measurement in steep stream channels.

This study seeks to develop new insights into the hydraulics of step-pool channels using detailed three-dimensional measurements of velocity structure and turbulence characteristics in a small step-pool channel in the Colorado Rockies. We investigate how three-dimensional velocity structure and turbulence features vary with discharge, are controlled by step-pool bed morphology, and differ from lower-gradient systems. This research builds on the work of Wohl and Thompson (2000) by using three-dimensional measurement methods in the same step-pool channel they examined. Our study employs a recently developed three-dimensional current meter, the SonTek FlowTracker Handheld ADV, and is the first study that we are aware of that has used the FlowTracker ADV or any other acoustic Doppler method to characterize hydraulics in a high-gradient stream channel (although see

Legleiter et al. (2007) for a FlowTracker application in a pool-riffle channel). The usefulness of this instrument for studies of velocity and turbulence in steep channels is evaluated below.

## 2. Methods

### 2.1. Field area

Data collection was completed on a 30 m step-pool reach of East St. Louis Creek, which is located in the Colorado Rockies approximately 80 km west of Denver,

CO, in the Fraser Experimental Forest (Fig. 1). Discharges have been recorded since 1943 at a gauging station maintained by the U.S. Forest Service that is located approximately 300 m downstream from the study reach. Discharge data show that East St. Louis Creek has a snowmelt-driven hydrologic regime, with average peak discharges occurring in mid-June and 80% of total flows occurring between April and October. East St. Louis Creek is characterized by a low sediment supply, cold temperate climate (mean annual precipitation of 740 mm) (Alexander et al., 1985), and relatively abundant large woody debris (LWD) compared to many

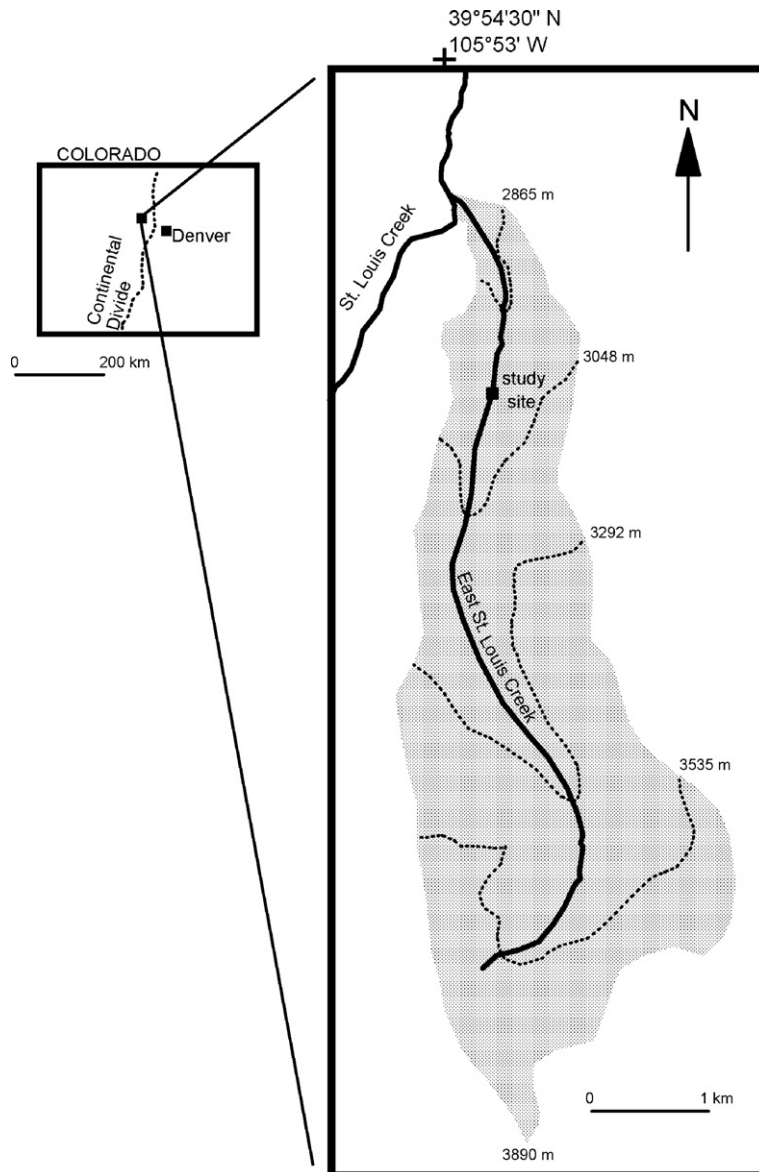


Fig. 1. East St. Louis Creek location map. Study reach is located at approximately 2930 m elevation.

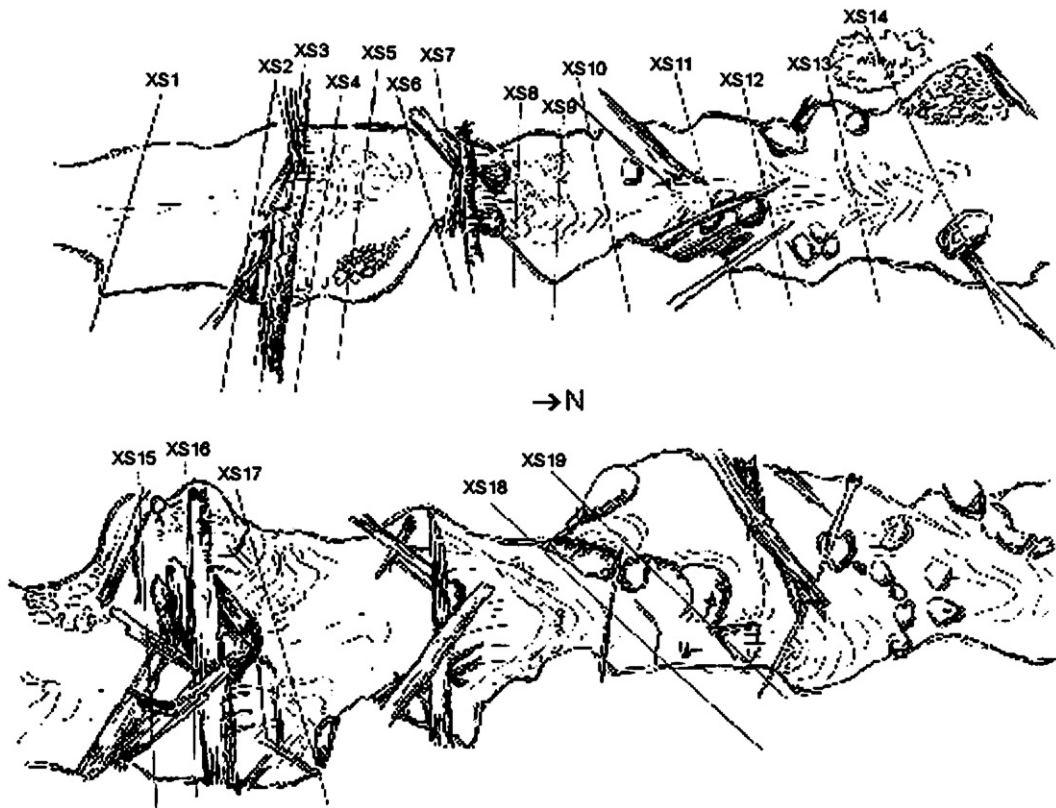


Fig. 2. Sketch of study reach showing step-pool sequences and cross-sections along which velocity was measured; flow is from left to right, and right side of upper sketch approximately connects with left side of bottom sketch. Channel length depicted here is 30m; average channel width is approximately 4m (sketch by Julie Kray).

streams in the Colorado Rockies. LWD dynamics may have been altered by limited timber harvest in the vicinity of the study reach in the early 20th century, although the upstream drainage area has been largely undisturbed by anthropogenic land uses. The study reach encompasses four distinct step-pool sequences, including log steps and boulder steps (Figs. 2–4).

Additional characteristics of the study reach are shown in Table 1.

## 2.2. Field measurements

Repeat measurements of three-dimensional velocity profiles were performed across a range of discharges at various positions representative of bedforms found in steep channels. These positions are: (1) above step (locations approximately 0.5m upstream from step lips and typically characterized by a reverse approach gradient and gravel/cobble substrates), (2) step lip (locations formed by boulders and/or LWD as close to the crest or brink of steps as was measurable with the velocity meter), (3) base of step (at the base of the step riser, where flow from the step lands; generally 0.5–1m downstream from the step lip), (4) pool (in the zone of accelerating flow downstream of the hydraulic boil in pools; generally 0.5m downstream from base-of-step positions), (5) cascades (areas with tumbling flow but lacking pools), and (6) run (lower-gradient portions of the study reach). Nineteen cross-sections

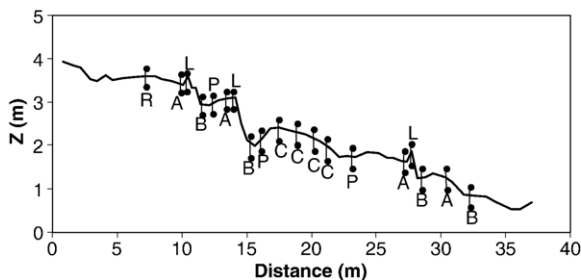


Fig. 3. Thalweg longitudinal profile of East St. Louis Creek study reach. Cross-section locations are shown by vertical bars and represent different morphologic positions, as follows: R=Run, A=Above step, L=Step lip, B=Base of step, P=Pool, C=Cascade. Cross-sections correspond to those depicted in Fig. 2.



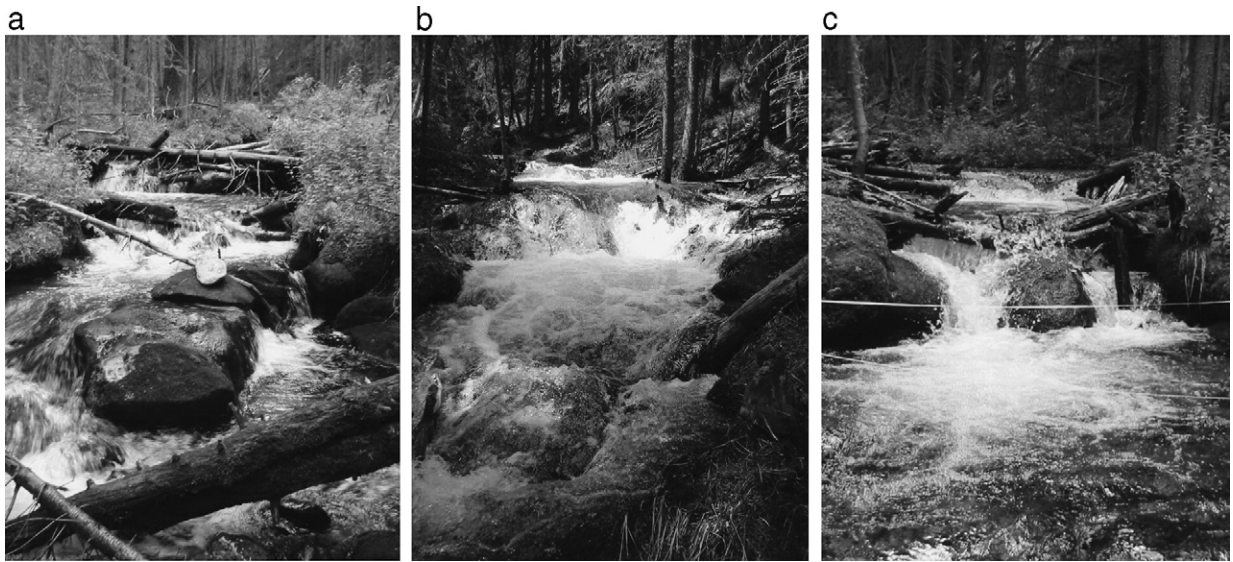


Fig. 4. Downstream portion of East St. Louis Creek study reach at  $Q(\text{discharge})=0.13 \text{ m}^3/\text{s}$  (a) and upstream portion of study reach at  $Q=0.60 \text{ m}^3/\text{s}$  (b) and  $Q=0.13 \text{ m}^3/\text{s}$  (c).

were established in positions representative of each of these morphologies (Table 2, Figs. 2–4).

Velocity measurements were repeated at each position during five different discharge periods (Table 3). The study period (2001–2003) coincided with a multi-year drought, skewing the range of sampled discharges downward. Discharges during each measurement period were determined using hourly flow data from the U.S. Forest Service gage located downstream from the study reach and were compared to the mean annual flow of  $0.76 \text{ m}^3/\text{s}$  from 1943 to 2003. Measurements during snowmelt periods, especially in June 2001, were subject to diurnal and inter-daily fluctuations in discharges (Table 3).

During all five measurement periods, a thalweg velocity profile, consisting of at least three points in the water column, was collected along each monumented cross-section. Additional non-thalweg profiles were also measured along each cross-section during three of the measurement periods to assess lateral variations in hydraulics. To facilitate the analyses of variations in

hydraulics with discharge and morphologic positions that are a central focus of this paper, the data presented here are derived from thalweg-only measurements. Measurement positions were relocated during each data-collection period based on distances from rebar benchmarks placed on one bank of each cross-section. During the moderately high-flow data collection period, measurements were taken at  $z/h=0.2, 0.6, \text{ and } 0.8$ , where  $z$  is position in the water column and  $h$  is local flow depth (modified from Byrd et al., 2000; USGS, 1977). During all other field efforts, vertical velocity profiles, consisting of 4–8 data points, were measured at linear intervals of  $0.1h-0.2h$ . Although concentrating measurements in the near-bed region would have facilitated analysis of Reynolds stresses, instrument limitations precluded this approach, as discussed further below.

1-Hz time series of either 180s (moderately high- and moderate-flow data collection periods) or 90s (all other periods) were measured at each position.

Table 1  
Summary of East St. Louis Creek study reach characteristics

Gradient	0.10 m/m
Average bankfull width	4.2 m
Drainage area	8 km <sup>2</sup>
Average elevation	2930 m
Grain size (reach composite)	$D_{50}=78 \text{ mm}$ $D_{84}=260 \text{ mm}$
Average step height ( $H$ )	0.5 m
Average step length ( $L$ )	4.3 m

Table 2  
Positions surveyed to characterize effects of morphology on hydraulics, and cross-sections associated with each morphologic position

Morphologic position	Cross-section
Above step	2,6,15,18
Step lip	3,7,16
Base of step	4,8,17,19
Pool	5,9,14
Cascade	10–13
Run	1

Table 3  
East St. Louis Creek discharge during field data collection periods, based on data from U.S. Forest Service gauging station

Measurement period	Discharge range (m <sup>3</sup> /s)	Average percent of mean annual flow	Date
High	0.58–0.64	80	June 2003
Moderately high	0.29–0.41	45	June 2001
Moderate	0.12–0.15	17	July 2001
Low	0.075–0.08	10	June 2002
Very low	0.054–0.058	7	August–September 2001

Buffin-Belanger and Roy, (2005) found that 60–90 s time series are typically sufficient in length to capture turbulence characteristics for high-frequency (20–25 Hz) instruments. Their suggested duration comprises a much larger number of time steps than we measured, however, because of the lower frequency (1 Hz) of our measurement device. Our record lengths were selected in part as a compromise between record length and number of sampling points.

Cross-section and longitudinal-profile (water surface and thalweg) surveys were completed using a total station to characterize channel geometry and local- and reach-average gradients. Pebble counts were completed during the low-flow field period using a transect method to characterize grain sizes (Table 1). Complete survey results are presented in Wilcox (2005).

### 2.3. Instrumentation

Velocity was measured using a SonTek FlowTracker Handheld ADV (Version 2.0), which records streamwise, cross-stream, and vertical velocity components (SonTek, 2001). The FlowTracker ADV has a sideways-facing probe that measures a 0.25 cm<sup>3</sup> sampling volume located 10 cm away to the side of the instrument. The FlowTracker reports velocities in *x–y–z* coordinates relative to the probe orientation, where, with the probe oriented with the *x*-axis downstream, *x* is the streamwise direction (positive downstream), *y* is the cross-stream direction (positive towards the left bank), and *z* is vertical (positive upward). We denote the streamwise, cross-stream, and vertical velocities as *u*, *v*, and *w*, respectively.

Acoustic Doppler velocimeters measure flow velocity by transmitting an acoustic pulse that bounces off suspended sediment, air bubbles or other scattering particles in the flow and back to the instrument; velocity is recorded based on the resulting frequency shift in the transmitted signal. Signal-to-noise ratio (SNR), which is

recorded by the FlowTracker for each velocity reading, measures the strength of the reflected acoustic signal compared to instrument noise and is largely a function of whether sufficient particulate matter is present in the water (SonTek, 2001). The principles of operation for ADVs have been described elsewhere (Lane et al., 1998; Nikora and Goring, 1998; McLelland and Nicholas, 2000), although the FlowTracker differs in important respects from other ADVs. Those ADVs record velocities at higher frequencies (up to 100 Hz) than the FlowTracker, increasing the suitability for turbulence analysis; report correlation, a data-quality metric that facilitates post-processing data filtering (Wahl, 2000); allow programming of velocity ranges; and have smaller sampling volumes. We selected the FlowTracker for this study because of our desire to generate three-dimensional data and because the FlowTracker has several field-deployment advantages over other ADVs. The FlowTracker can be mounted on a standard top-setting rod, is suitable for operation in shallow flows because of its sideways-facing probe, does not require an external power source or data-logger, and is smaller and lighter than other ADVs.

### 2.4. Data analysis

Each velocity measurement was separated into mean and fluctuating components by Reynolds decomposition; for example:  $u = U + u'$ , where *u* is the instantaneous (1-s) streamwise velocity, *U* is the mean streamwise velocity for a time series, and *u'* is the fluctuating component of the instantaneous velocity. Cross-stream and vertical velocities were similarly decomposed ( $v = V + v'$ ;  $w = W + w'$ ). Mean velocity components (*U*, *V*, *W*) were used to calculate the magnitude of the three-dimensional velocity vector ( $M_{uvw}$ ) for each time series:

$$M_{uvw} = \sqrt{U^2 + V^2 + W^2}. \quad (1)$$

The relative influence of each component on the velocity field was calculated by dividing  $U^2$ ,  $V^2$ , and  $W^2$ , respectively, by  $M_{uvw}^2$ .

Turbulence intensities which reflect the magnitude of the fluctuating components of velocity around the mean, were calculated as the root mean squares of the streamwise, cross-stream, and vertical velocities (RMS<sub>*u*</sub>, RMS<sub>*v*</sub>, RMS<sub>*w*</sub>) for each time series (Clifford and French, 1993; Middleton and Wilcock, 1994). To facilitate comparisons of turbulence intensities between measurement locations and periods, dimensionless RMS values, denoted RMS'<sub>*u*</sub>, RMS'<sub>*v*</sub>, and RMS'<sub>*w*</sub>, were

calculated by dividing each RMS component by  $M_{uvw}$ . In addition, to represent overall, three-dimensional turbulence intensity, average turbulent kinetic energy density (TKE) was calculated for each time series (Clifford and French, 1993):

$$\text{TKE} = \frac{1}{2} \rho (\text{RMS}_u^2 + \text{RMS}_v^2 + \text{RMS}_w^2), \quad (2)$$

where  $\rho$  is the fluid-mixture density (assumed to equal  $1000 \text{ kg/m}^3$ ) and TKE has units of  $\text{N/m}^2$ . Similar to the manner in which the relative influences of  $U$ ,  $V$ , and  $W$  on the velocity field were calculated, we calculated the contributions of the turbulence intensity in the stream-wise, cross-stream, and vertical components to TKE by dividing each squared RMS component (multiplied by  $0.5 * \rho$ ) by TKE.

Because of limitations associated with the FlowTracker ADV, including its sampling frequency (1 Hz) and its poor performance in near-bed environments, as discussed in Section 4, we confined our turbulence analysis to RMS and TKE. More detailed analysis of turbulence may include calculation of Reynolds shear stresses, characteristic length scales of turbulence features, spectral properties, and quadrant analysis of deviatoric velocity terms to characterize turbulence event structure (Clifford and French, 1993; Nezu and Nakagawa, 1993).

For comparisons between discharge periods and morphologic positions, vertical averages of velocity and turbulence intensity were calculated for each profile using Riemann averaging. Averages over discharge or morphologic position used absolute values of  $V$ , because the sign of cross-stream velocities (i.e., whether these values indicated flow toward the left bank or the right bank) was not important in this analysis and retaining the sign would bias averages toward zero. Froude numbers were calculated for each velocity profile based on vertically averaged downstream velocities ( $U$ ) and flow depth.

Analyses of variance (ANOVA) were completed to assess the influence of morphologic position and discharge on three-dimensional mean velocity, RMS, RMS', TKE, and Froude number values. Log transformations were applied to values of RMS and TKE to stabilize variances. For the analysis of variance, we treated our data collection as a repeated measures design and a mixed random-effects model was used, whereby morphology was treated as a random blocking effect and each cross-section position was assigned to blocks. A Satterthwaite approximation was applied in the mixed effects model for computing the denominator degrees of freedom in tests of fixed effects (SAS, 2004). ANOVAs

testing the effect of morphologic position provided a means of evaluating the relative magnitudes of variability within each morphologic position grouping (e.g., among the four above-step measurement positions listed in Table 2) versus variability between morphologic positions (e.g., above step versus base of step).

For the purposes of statistical analyses, we assumed that discharge was fixed during each field measurement period and used the average discharge during each period in statistical models. Discharge variations that occurred during these field sessions (Table 3) introduced variability that was not explicitly accounted for in our statistical models, thereby reducing significance levels.

### 2.5. Data filtering

Because the FlowTracker produces erroneous data in certain measurement environments, data filtering was an important initial component of data analysis. Filtering was necessary to eliminate data that may have been compromised as a result of factors such as obstructions within or near the sampling volume (particularly with respect to near-bed measurements), excessive aeration of flows, proximity to the surface, and/or difficult measurement positions; these topics are discussed further in Section 4.

We adopted a conservative, multi-step approach to data filtering. First, individual 1-s velocity measurements with mean SNR values  $<10$  dB and  $>35$  dB were removed, based on the manufacturer's recommendation for optimal operating conditions (SonTek, 2001) and on our initial data analysis. Next, individual measurement points more than 3 standard deviations away from the SNR-filtered mean ("spikes") were removed. If velocity readings for either the  $u$  or  $v$  components were filtered by the above methods, the remaining velocity components were also excluded. In cases where only the  $w$  data were removed, however,  $u$  and  $v$  data were retained. The processing algorithm for the FlowTracker allows it to record valid  $u$  and  $v$  data even when  $w$  data are corrupted, but not vice versa (Huhta, 2003). Time series in which more than half of the individual data points were removed by SNR- and spike-filtering were automatically excluded from further analysis. To avoid artificially reducing RMS values, we did not substitute time-series means or other data for filtered points.

We also removed all time series from further analysis in which any one of the three dimensionless RMS values were greater than five. Time series exceeding this threshold typically consisted of near-zero mean velocities with very large fluctuations, suggesting that

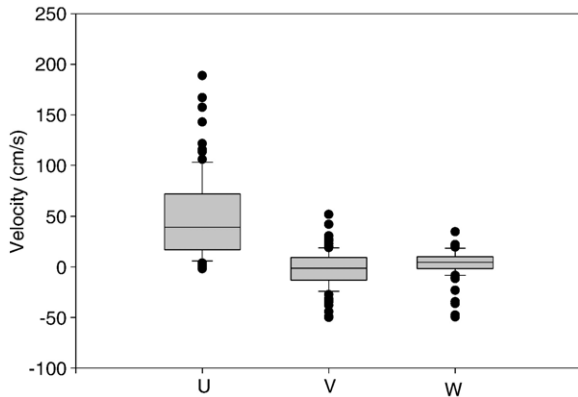


Fig. 5. Distribution of vertically averaged mean streamwise ( $U$ ), cross-stream ( $V$ ) and vertical ( $W$ ) velocities for thalweg positions at multiple morphologic positions and discharges in East St. Louis Creek study reach. Here and in Figs. 7, 8, and 14, boxes represent 25th–75th percentiles, error bars above and below boxes show 10th and 90th percentiles, and black circles represent velocities outside of the 10th–90th percentile range.

constituent data were likely erroneous. In addition, time series in which the standard deviation of recorded SNRs was zero were removed because of the likelihood that such time series were corrupted (Huhta, 2003).

Because erroneous data can result from factors that are not measured by SNR and can produce standard deviations large enough to limit the effectiveness of spike filtering, we also manually filtered individual data points and/or time series that appeared erroneous following visual inspection. Manual filtering was performed after review of numerous time series suggested characteristic patterns of erroneous data produced by the FlowTracker, as discussed further in Section 4. Because of the large volume of data originally collected, sufficient data remained to address the study objectives even after extensive filtering.

During field measurements, we attempted to align the FlowTracker so that its frame of reference was parallel to flow streamlines, which was equivalent in most but not all cases to a perpendicular alignment with respect to cross-sections. Based on the complexity of the flow field in our study reach and the likelihood that deviations of mean vertical velocity from zero result primarily from velocity vector orientation rather than sensor misalignment, no rotation was applied to our instantaneous velocity measurements (Roy et al., 1996). Further, because the FlowTracker reports velocities in  $x$ – $y$ – $z$  coordinates relative to the probe orientation, no rotation of velocity data is required if the probe is oriented with the  $x$ -axis pointed downstream (Huhta, 2003).

Additional assessment of the quality of FlowTracker velocity data, based on comparisons with other methods of measuring local and reach-averaged velocity in East St. Louis Creek, is presented in Wilcox (2005).

### 3. Results

#### 3.1. Overview

The distribution of streamwise ( $U$ ), cross-stream ( $V$ ), and vertical ( $W$ ) thalweg velocities measured here are shown in Fig. 5, which illustrates the variability resulting from differences in morphologic position and discharge and the relative magnitudes of  $U$ ,  $V$ , and  $W$  with respect to each other. Analysis of the relative influence of each velocity component on  $M_{uvw}$  indicated that streamwise velocities were the largest-magnitude components of the velocity field, contributing slightly less than two-thirds of the overall velocity vector magnitude. Mean cross-stream and vertical velocities contributed an average of 20% and 15% of the overall vector magnitude, respectively, averaging across discharges and morphologic positions. Linear regressions indicated that  $U$ ,  $V$ , and  $W$  values were poorly correlated with each other ( $r^2 < 0.10$ ). In contrast,  $RMS_u$ ,  $RMS_v$ , and  $RMS_w$  values were all well correlated with each other, particularly  $RMS_u$  and  $RMS_w$  ( $r^2 = 0.72$ ) and  $RMS_u$  and  $RMS_v$  ( $r^2 = 0.76$ ) (Fig. 6).

Mean values of dimensionless  $RMS_u$ ,  $RMS_v$ , and  $RMS_w$  for thalweg velocity profiles were 0.7, 0.4, and 0.9, respectively (medians = 0.5, 0.3, 0.6, respectively). This indicates that RMS values of the same order of magnitude as the overall velocity vector magnitude were typical, and that turbulence intensities that were larger than mean velocities were not uncommon (Fig.

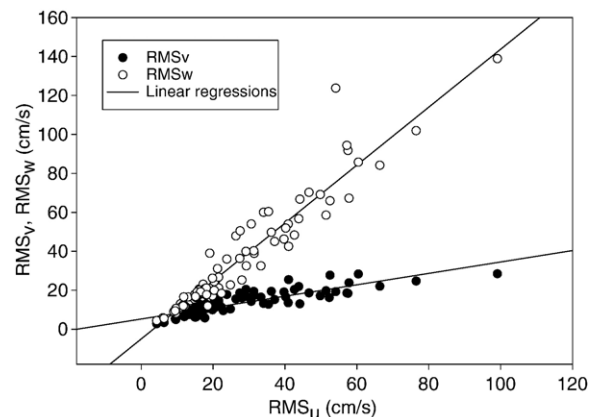


Fig. 6. Linear regression of unstandardized turbulence intensities:  $RMS_u$  versus  $RMS_v$  and  $RMS_w$ .



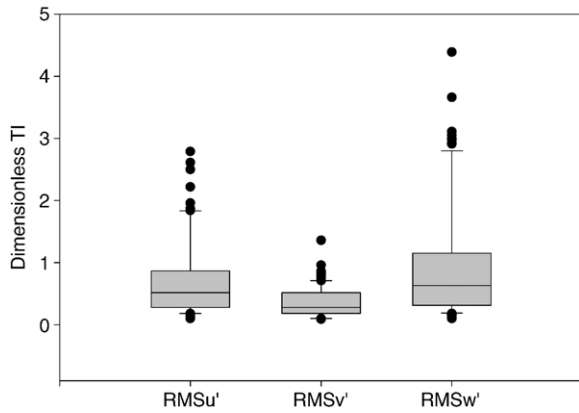


Fig. 7. Distributions of measured dimensionless turbulence intensity (TI) for each of three velocity components ( $RMS'_u$ ,  $RMS'_v$ ,  $RMS'_w$ ), where  $RMS'$  consists of RMS divided by velocity vector magnitude.

6). Turbulence intensities in the vertical component ( $RMS_w$ ), including unstandardized and dimensionless values, were higher than in the streamwise and cross-stream components for nearly all measurement positions (Figs. 6 and 7). This result may partly reflect the tendency of the FlowTracker to produce greater instrument noise in the vertical component than in the downstream component, as discussed in Section 4.2. Turbulence intensities in the cross-stream velocity component were small compared to those in the streamwise and vertical components (Figs. 6 and 7).

### 3.2. Effects of morphologic position

Analyses of variance indicated that the effect of morphologic position was significant in the streamwise velocity component ( $U$ ), but not in the cross-stream ( $V$ ) and vertical ( $W$ ) components (Table 4). In particular, significant differences in  $U$  were found between positions upstream from steps (above steps, step lips) versus downstream from steps (base of steps, pools).  $U$  measured in runs was significantly different than that in positions downstream from steps but not other positions. The ANOVA results illustrate that the variability in  $U$  within most of the morphologic position groupings (e.g.,

between different above-step positions in the study reach) is small compared to the variability in  $U$  between morphologic positions.

The variation in the pattern of mean velocity with morphologic position, which is evident in the overall velocity vector magnitude (Fig. 8) and in  $U$  (Fig. 9), reflects the acceleration and deceleration caused by step-pool structures. Flow gains velocity along step treads until it reaches a maximum at the step lip, after which it plunges into downstream pool positions and decelerates sharply, before again repeating the sequence; intermediate velocities occur in runs and cascades.

Spatial variations in the relative magnitude of  $U$  and  $W$  components with respect to each other, and in relative contribution to velocity vector magnitude, were also evident between morphologic positions. For example, the average of  $W$  values in base-of-step positions was 50% as large as the average of  $U$  values, whereas average  $W$  was only 8% as large as average  $U$  in above-step positions.

Although vertical velocities were not significantly different between morphologic positions, qualitative differences were evident (Fig. 9). At most positions, vertically averaged values of  $W$  were small but positive, averaging 2–6 cm/s and indicating weak flow away from the bed. At positions near step lips, in contrast, vertical velocities were typically negative, indicating flow towards the bed and/or downwards towards the overfall of plunging flow over the step lip. Absolute values of cross-stream velocities were higher upstream of steps than in other positions, potentially reflecting steering of the flow by step-forming obstructions, although this effect was not statistically significant.

All dimensionless components of RMS were significantly affected by morphologic positions in the analyses of variance, although morphology effects on unstandardized values of RMS were not significant (Table 4), reflecting the large variation in values of RMS within each morphologic position. Values of RMS show the opposite spatial pattern of mean streamwise velocities, with high RMS values occurring at positions where velocities are low (at the base of steps and in

Table 4  
Summary of analyses of variance testing effects of morphology, discharge ( $Q$ ), and two-way morphology\*discharge interactions on hydraulic parameters

Effect	$U$	$V$	$W$	$RMS_u$	$RMS_v$	$RMS_w$	$RMS'_u$	$RMS'_v$	$RMS'_w$	TKE	$Fr$
Morphology	0.003	0.33	0.30	0.08	0.04	0.22	0.004	0.007	0.02	0.16	0.0005
$Q$	<0.0001	0.10	0.21	<0.0001	<0.0001	<0.0001	0.88	0.86	0.98	<0.0001	0.004
Morphology* $Q$	0.83	0.09	0.31	0.70	0.65	0.88	0.95	0.67	0.95	0.86	0.34

Values shown are  $p$ -values produced by analyses of variance using mixed random-effects models.

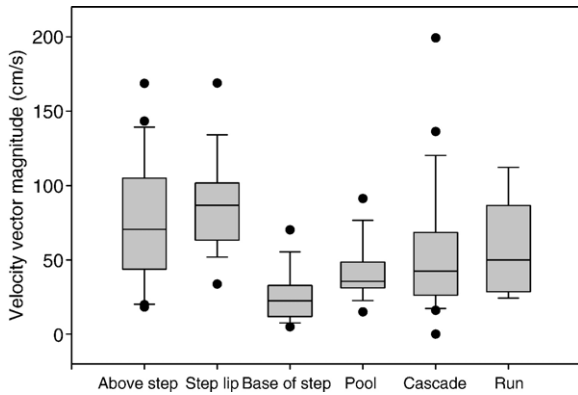


Fig. 8. Distribution of velocity vector magnitudes at different morphologic positions, combining cross-section positions and measurement periods.

pools) and low RMS values coinciding with high velocity positions (upstream from steps, step lips, runs) (Fig. 10).

3.3. Temporal variations

A highly significant discharge effect on  $U$  was observed in the analysis of variance (Table 4), with  $U$  consistently increasing with discharge (Fig. 11). Discharge did not significantly affect  $V$  or  $W$ , and no consistent pattern of temporal variation was observed in  $V$  and  $W$  (Fig. 11). The increase of  $U$  with  $Q$  was expected because of the collinearity between  $U$  and  $Q$  in a velocity field where the overall velocity vector magnitude is controlled by the streamwise component and because channel geometry in East St. Louis Creek

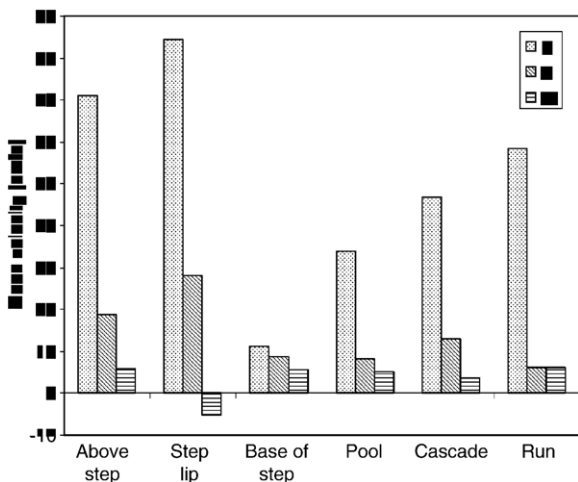


Fig. 9. Variation in mean velocities ( $U$ ,  $V$ ,  $W$ ) with morphologic position, averaged over all discharges.

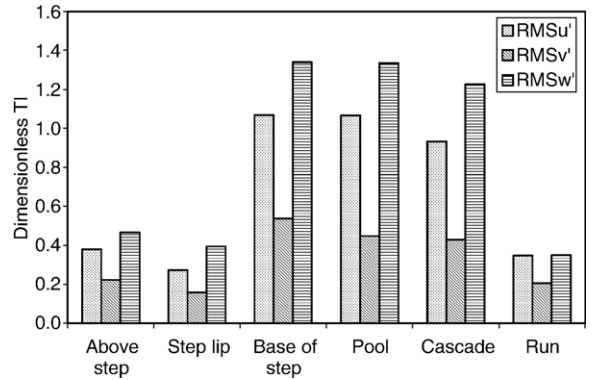


Fig. 10. Variation in dimensionless turbulence intensity ( $RMS_{u'}$ ,  $RMS_{v'}$ ,  $RMS_{w'}$ ) with morphologic position, averaged over all discharges.

dictates that changes in discharge are accommodated largely by changes in velocity and depth up to the bankfull level. The response of  $V$  and  $W$  to changes in  $Q$  was less predictable, however because of the potential influence of changes in relative submergence with changing  $Q$  on local patterns in these velocity components.

The effect of discharge on unstandardized turbulence intensities was highly significant (Table 4) for all flow components, with RMS values in all velocity components decreasing consistently with  $Q$ . Discharge, however, did not significantly affect any of the dimensionless RMS components (Fig. 12). Dimensionless turbulence intensities tended to be highest during the lowest-discharge measurement period, but no consistent pattern of variation in dimensionless RMS

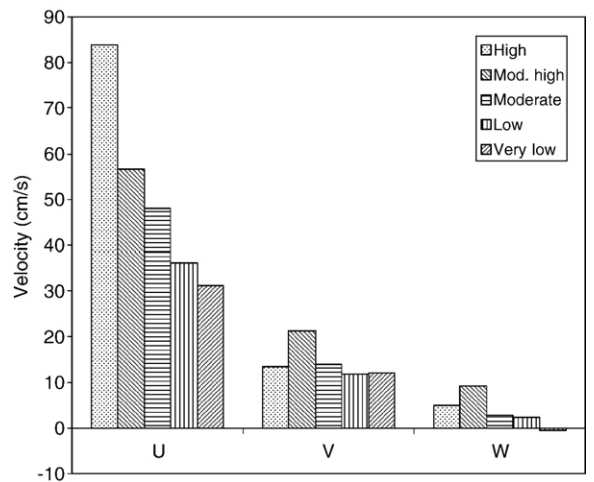


Fig. 11. Mean velocities ( $U$ ,  $V$ ,  $W$ ) at five discharges, averaged over morphologic position.

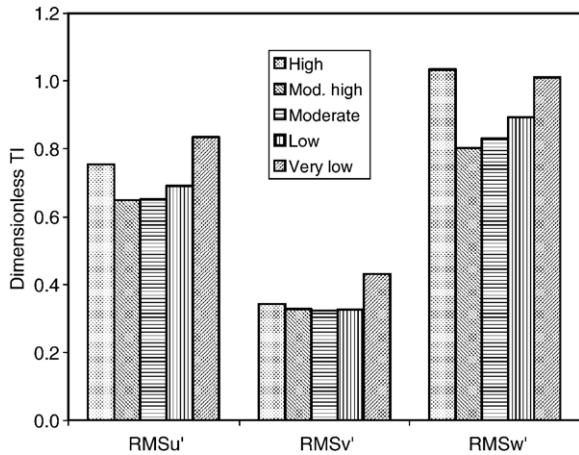


Fig. 12. Dimensionless turbulence intensity (RMS') for each of three velocity components at five discharges.

with  $Q$  was evident (Fig. 12). This suggests that the increase in turbulence with discharge is largely driven by increases in velocity, but that the size of fluctuating components compared to mean components of velocity does not change significantly with discharge. Interaction effects between discharge and morphologic position were not significant at  $\alpha=0.10$  for any components of velocity or RMS.

Turbulent kinetic energy displayed similar patterns to those shown by the individual (unstandardized) RMS components (Table 4), as would be expected because TKE is calculated using  $RMS_u$ ,  $RMS_v$ , and  $RMS_w$  (Eq. (2)). At most morphologic positions, TKE decreased consistently with  $Q$ , although consistent patterns in TKE were not observed for step-lip and base-of-step positions. Very large values of TKE were measured in pools and cascades (Fig. 13).

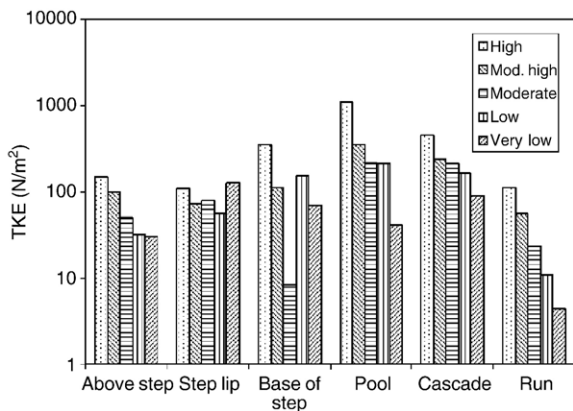


Fig. 13. Average turbulent kinetic energy density (TKE) versus discharge, by morphologic position.

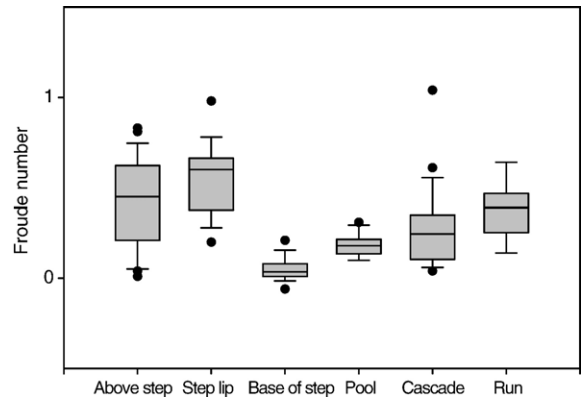


Fig. 14. Variation in Froude number with morphologic position, averaged over discharge. These data suggest that flows are subcritical in nearly all measured positions in East St. Louis Creek, although supercritical flow was visually observed in unmeasurable positions.

Calculation of the relative contributions of  $RMS_u$ ,  $RMS_v$ , and  $RMS_w$  to TKE indicated that turbulence in the streamwise, cross-stream, and vertical velocity components contributed an average of 36%, 13%, and 51% of TKE, respectively, averaging over our measurement positions. The contributions of  $RMS_u$  and  $RMS_w$  to TKE may be more similar than these values suggest, however, because of noise inflation by the FlowTracker ADV in the vertical component (as discussed further in Section 4.2). Minimal variation in the relative contributions to TKE was observed between discharge periods.

### 3.4. Froude number

Froude numbers were less than 1 at all measurement locations except one (Fig. 14), including at high flows and in high-velocity measurement positions (above steps and at step lips). Locations of apparent supercritical flow were observed visually, particularly at the true crest or brink of steps. These locations were typically slightly downstream of our “step-lip” positions and were not measurable with the FlowTracker ADV because of shallow flow depths. Despite the local occurrence of supercritical flow and hydraulic jumps as flow plunges over step lips into downstream pools (Fig. 4), our data suggest that subcritical flow is spatially predominant in this step-pool channel in the wadable flow range.

## 4. Discussion

### 4.1. Three-dimensional hydraulics

Our results illustrate the substantial spatial variability in hydraulics in this channel, where positions upstream

from steps, which are associated with high velocities and low turbulence intensities, alternate with areas downstream from steps that are spatially proximal but hydraulically extremely different, having substantially lower velocities and much higher turbulence intensities. The grouping of RMS values between areas with high turbulence intensities (base of steps, pools, cascades) and areas with relatively low turbulence intensities (runs, above steps, near step lips) (Fig. 10) illustrate the interplay between morphology and energy losses in this channel.

Temporal variability in hydraulics during our study resulted primarily from discharge variations and to a lesser extent from morphologic changes. East St. Louis Creek is generally a stable channel, partly as a result of its low sediment supply and a snowmelt-driven hydrologic regime in which flashy high-flows are rare. Our study design assumed that morphologic changes would be minimal between study periods, allowing repeat measurements in the same positions that would represent only the effects of changing discharges. During the first 2 years of this study (2001–2002), which corresponded to a drought period in the study area, no morphologic changes were visibly evident in the study reach. The final data-collection period corresponding to the highest flow that we measured (Table 2), followed an above-bankfull event that caused the partial breaching of one of the log steps in the study reach (as is visible in the upstream-most step in Fig. 4b and c) and shifting of a step-forming log in a second step. At the breached step (cross-section 3), evidence of the effect of the reduction in drag at this step is provided by a doubling of the velocity vector magnitude, from 0.85 m/s to 1.7 m/s, between the moderately high and high discharge periods (Table 3), a substantially greater rate of increase than was observed at other positions between these periods.

We expected that increasing discharge would reduce the effect of bed morphology on average velocities and turbulence intensities even in the absence of the type of flow-induced morphologic changes observed at cross-section 3. At higher discharges in step-pool channels, steps and other roughness features are drowned out and water surface profiles become more smooth, with the height of overfalls over steps decreasing (Chin, 2003). Flume studies examining the flow resistance dynamics in step-pool channels have quantified the effect of increasing discharges on bed roughness in terms strong two-way interactions between  $Q$  and bed roughness features (i.e., model LWD and steps) (Wilcox, 2005; Wilcox and Wohl, 2006). We tested this effect in East St. Louis Creek as well using two-way ANOVAs to

examine the morphology\* $Q$  interaction effect on mean velocity components and turbulence intensities. Such an interaction effect could be viewed as analogous to the velocity convergence effect that has been observed in pool-riffle channels, where velocity differences between pools and riffles decrease as flow increases (Keller and Melhorn, 1978). No statistically significant interaction effects, however, were observed between morphologic position and  $Q$  on any of the hydraulic parameters that we measured (Table 4). This may be because a sufficiently large range of discharges was not measured, although it is more likely that the considerable variability in FlowTracker ADV data between measurement positions and periods reduced the significance of any interaction effect.

Qualitative assessment of our study reach suggests that the effect of bed morphology on hydraulics did change with discharge, despite the lack of statistical significance for this effect. For example, Figs. 4b and c illustrate how step-pool sequences are submerged as stage increases. At low flows, these features generate substantial localized turbulence as flow plunges over steps and decelerates in downstream pools, whereas at higher flows, velocities and the turbulence intensities are consistently higher throughout the channel, with less variation caused by underlying bedforms. Further, several small step-pool features in the study reach that are evident at low discharges are completely drowned out at higher flows, assuming a more cascade-like morphology. This includes several of the measurement locations that we classified as cascades (cross-sections 12 and 13).

The presence of non-negligible vertical and cross-stream velocities illustrates the substantial contributions of roller eddies, lateral eddies, and other non-streamwise flow to flow structure. We expected that, because of the effect of plunging flow over steps and upwelling in pools, vertical velocity components would constitute an important part of the flow field. This was indeed the case, as mean velocities in the vertical contributed an average of 15% to overall velocity vector magnitudes. Vertical velocities had an even greater influence locally, indicating flow movement towards or away from the bed in areas of plunging and upwelling flow. The relatively large average contribution of cross-stream velocity components (20%) to  $M_{uvw}$  was unexpected, however, given the relatively straight nature of our study reach. As discussed in Section 2.5, we did not apply a rotation to our velocity data, and the possibility that  $V$  and  $W$  components were inflated as a result of sensor misalignment cannot be discounted. Furthermore, the common application of a rotation to three-dimensional



velocity data in lower-gradient systems limits the availability of comparable data regarding the relative contributions of cross-stream and vertical velocities to flow structure. Our quantification of the contributions of  $V$  and  $W$  to vector magnitudes does, however, suggest a potential source of error in one-dimensional methods of computational modeling in step-pool channels.

We also found that turbulence intensities in the vertical velocity component were an important contributor to turbulence in our study reach. Studies in lower-gradient systems, as reviewed by Sukhodolov et al. (1998), often have assumed that the contribution of streamwise velocity to TKE amounts to 60–80%. Sukhodolov et al. (1998) found that the streamwise component is responsible for 45–55% of TKE, irrespective of flow depth. They found that the remaining contributions from the cross-stream and vertical components varied with depth, with the vertical component lowest near the bed and the surface, and mid-profile contributions to TKE averaging approximately 20% and 30% in the vertical and cross-stream components, respectively. We found that TKE contributions from streamwise velocities are smaller (an average of 36% in our study reach, averaging over our measurement positions), whereas turbulence in the vertical velocity component contributes approximately half of TKE. Furthermore, we did not observe any obvious vertical variation within the water column in the relative contributions of  $RMS_u$ ,  $RMS_v$ , or  $RMS_w$  to TKE. Although values of RMS in the vertical velocity component may be inflated by instrument noise, as discussed below, the general conclusion regarding the multi-dimensional contributions to turbulence in our channel is likely valid.

The turbulence intensities measured in East St. Louis Creek, as represented by dimensionless values of RMS, were very large compared to low-gradient channels. Whereas we found that, on average, RMS values were between 50% and 100% of overall velocity vector magnitudes, limited data from lower-gradient rivers suggest that turbulence intensities are typically on the order of 5% to 20% of mean velocity values (Middleton and Southard, 1984; Sukhodolov et al., 1998).

Our results characterizing Froude numbers add to the body of data on the prevalence of supercritical ( $Fr > 1$ ) flows in step-pool channels. Peterson and Mohanty's (1960) description of tumbling flow regimes suggests that supercritical flows are typical upstream from steps, and descriptions of step-pool channels often refer to the presence of supercritical flows. Grant (1997) reviews data on Froude numbers and hypothesizes that interactions between hydraulics and bedforms maintain com-

petent flows to  $Fr \leq 1$  in step-pool and other channels. In East St. Louis Creek, hydraulic jumps were evident in our study reach and supercritical flow was likely present in positions that were not measured (e.g., in plunging flow jets and in shallow near-lip flows). Our measured values of Froude numbers, however, were in the subcritical range ( $Fr < 1$ ) at all positions except one (within a cascade bedform), even in positions upstream from steps with high ( $> 1$  m/s) flow velocities. These data suggest that, despite locally high flow velocities, the drag created by coarse substrates, step-pool structure, and woody debris increases flow depth sufficiently to maintain flow in the subcritical range across a large majority of the area of East St. Louis Creek.

#### 4.2. Evaluation of FlowTracker ADV

In our study reach, the FlowTracker ADV operated most effectively in flows with depths greater than 10 cm, low to moderate aeration, and in mid-profile regions. In terms of the morphologic positions sampled here, data quality was most consistent in runs and positions upstream from steps. The FlowTracker ADV performed poorly in certain environments, however, and produced several characteristic data problems, necessitating the intensive and time-consuming filtering procedure described above.

Questionable data were characterized by large fluctuations in instantaneous velocity measurements around the mean (i.e., large RMS values, see Fig. 15 for example), and often by low (near-zero) mean velocities. Such problems persisted even after SNR- and spike-filtering in some cases. Noise can be produced by acoustic Doppler methods as a result of difficulties in resolving the phase shift of return acoustic pulses to the

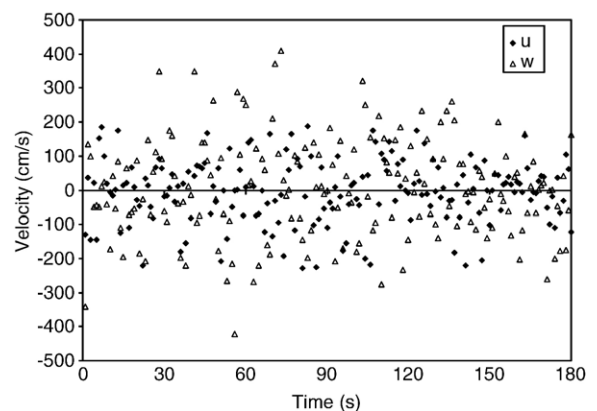


Fig. 15. Time series characterized by low mean velocities and very large values of RMS (only  $u$  and  $w$  components are shown to facilitate interpretation).

instrument, random scatter motions within the sampling volume (i.e., Doppler noise), velocity gradients within the sampling volume, and boundary interference (Lane et al., 1998; Voulgaris and Trowbridge, 1998).

In highly aerated positions, especially in pools below steps and/or near the surface, the FlowTracker often produced poor or ambiguous data. Determining whether the high values of RMS recorded in these positions represented real turbulence or instrument noise was often difficult. Acoustic Doppler methods are particularly susceptible to data problems in aerated flows because ADVs rely on the assumption that scattering particles (e.g., air bubbles) in the flow are traveling at the same velocity as the overall flow, an assumption that breaks down at high air concentrations. Field methods for measuring the aeration of hydraulic jumps (Valle and Pasternack, 2002; *in press*) could potentially be useful, in conjunction with ADV measurements in aerated flows, to help define the aeration limits under which ADVs are able to collect valid data. Laboratory tests at air concentrations of up to 8% have shown that ADVs provide reasonable estimates of mean velocity at these relatively low aeration levels (Frizell, 2000). Other laboratory methods have been developed for measuring velocity at high aeration levels (Frizell et al., 1994; Matos et al., 2002), but application of such methods to field settings currently appears impractical.

Near-boundary measurements also frequently produced questionable data. Near the water surface, increased aeration and/or rapidly varying flow that intermittently exposed one or more of the instrument's probes caused sampling errors. In addition, data collection near the bed was often compromised by the presence of boulders, logs, or other submerged obstacles either within or close to the sampling volume. These obstacles were typically not visible from the surface and presence was inferred from data characterized by low ( $<10$ ) values of SNR and near-zero velocities. Where the sampling volume includes the boundary, the ADV measures the Doppler shift of boundary reflection, rather than reflection from particles in water. Stationary boundary objects bias measured velocities toward zero and produce noise by disrupting the ADV's signal processing algorithms (SonTek/YSI, 2001).

The FlowTracker also sometimes recorded erroneous data in areas where a strong positive streamwise velocity was evident in the field, particularly in shallow flows. For example, highly negative values of  $u$  (on the order of  $-1$  m/s) were sometimes recorded throughout the velocity profile near step lips despite the apparent physical implausibility of such flows. These types of errors occur as a result of velocity ambiguities or

aliasing, where the FlowTracker incorrectly interprets positive velocities as negative values and readings fluctuate between large positive and large negative values (Wahl, 2000; Huhta, 2003).

Low SNRs or suspiciously high RMS values were most often associated with the  $w$  component. This results partly from the asymmetry of the FlowTracker's probe configuration, which creates instrument noise in the vertical component that should be approximately 50% higher than in the downstream component (Huhta, 2003). Further, because the beam that records vertical velocities is oriented upward on the FlowTracker,  $w$  and  $RMS_w$  data were especially problematic in near-surface positions and shallow flows. Some of the results presented above with respect to the importance of turbulence intensities in the vertical direction are, therefore, likely affected to some extent by noise inflation of  $RMS_w$  values. FlowTracker noise in the downstream component is typically approximately four times greater than in the cross-stream component (Huhta, 2003).

Approximately 30% of the data that were originally collected were filtered and not used, including a substantial portion of data from base-of-step positions, where aeration was greatest. This exceeds the amount of data filtering reported in other studies; for example, Legleiter et al. (2007) filtered 8–20% of data collected using a FlowTracker in a riffle, and Elgar et al. (2001) filtered 8% of values collected using a high-frequency ADV with an upward-facing probe in a marine surf zone.

Our overall assessment of data quality suggests that, except for in positions at the base of steps, the FlowTracker ADV usually produced valid mean velocity data, particularly on a vertically averaged basis and following data filtering. Data on turbulence intensities produced by the FlowTracker appear to be more sensitive to instrument errors, however, particularly in the vertical component. These findings indicate that the FlowTracker is appropriate for illustrating spatial and temporal variations in three-dimensional mean velocities, even in a challenging field setting such as this one, but that patterns of turbulence intensity, documented by the FlowTracker should perhaps be viewed as more qualitative in nature.

Data on spatial and temporal patterns of Reynolds shear stresses, turbulence event structure, and length scales of turbulence features would provide additional insights into shear generation, sediment–transport mechanics, and morphology in steep mountain channels. Collection of such data would require instrumentation capable of two-dimensional or three-dimensional measurements at high frequencies in near-boundary and potentially aerated positions, which is not currently

available. The data on three-dimensional velocity and turbulence intensity reported here represent an advance over existing characterizations of flow in steep channels. Although the FlowTracker data are not adequate for the type of detailed turbulence analysis listed above, they do provide insights into spatial and temporal patterns of hydraulics and into the multi-dimensional nature of hydraulics in step-pool channels.

## 5. Conclusions

This study has characterized velocity and turbulence characteristics in a three-dimensional framework in East St. Louis Creek, the first such data set that we know of for a step-pool channel or for any other type of high-gradient ( $S > 0.05$  m/m) channel. Our data suggest that flow structure in step-pool channels is more three-dimensional than in lower-gradient systems, where streamwise velocities dominate overall velocity vector magnitudes and turbulence intensities (i.e., flow is more one-dimensional). In particular, the contributions of mean velocities and especially turbulence intensities in the vertical component to overall flow structure were found to be substantial. Whereas the non-streamwise components of velocity and turbulence intensity were found to be broadly important to flow structure, cross-stream and vertical components exhibited less variation than streamwise components with either morphology (i.e., spatially) or discharge (i.e., temporally). Largely as a result of variations in the streamwise component, our results illustrate the large spatial variations in hydraulics created by step-pool bedforms and the sensitivity of hydraulics in these channels to discharge variations, reflecting the rapid changes in relative submergence in these channels with discharge. Future research, which will likely require improved instrumentation, is needed to gain further insight into step-pool hydraulics comparable to results for lower-gradient systems. For example, interactions between large-scale turbulence structures, vortex shedding, and bedforms, which have been extensively examined in lower-gradient systems (e.g., Nelson et al., 1995; Roy et al., 2004), may be important in explaining sediment-transport processes and bedform development in step-pool channels and merit further study.

## Acknowledgments

This work was funded by the National Science Foundation grant EAR-9902440 to support the primary author's PhD research, NSF equipment grant EAR-9907048, an NSF grant (EAR-0097560) to Colorado

State University to support the Research Experiences for Undergraduates program, and a Geological Society of America Graduate Research Grant. Thanks to Julie Kray and Glen Vallance for field assistance, Tracy Phelps for assistance with data processing, Laurie Porth and Manuel Martinez (U.S. Forest Service) for discharge data and field support, and Craig Huhta (SonTek) for providing insights on the FlowTracker ADV. We also thank Anne Chin, Lee Harrison, Jonathan Nelson, and Greg Paster-nack for comments that greatly improved the manuscript.

## References

- Abrahams, A.D., Li, G., Atkinson, J.F., 1995. Step-pool streams—adjustment to maximum flow resistance. *Water Resources Research* 31 (10), 2593–2602.
- Alexander, R.R., et al., 1985. The Fraser Experimental Forest, Colorado: Research program and published research 1937–1985. USDA Forest Service General Technical Report RM-118. InFort Collins, CO.
- Buffin-Belanger, T., Roy, A.G., 1998. Effects of a pebble cluster on the turbulent structure of a depth-limited flow in a gravel-bed river. *Geomorphology* 25 (3–4), 249–267.
- Buffin-Belanger, T., Roy, A.G., 2005. 1 min in the life of a river: selecting the optimal record length for measurement of turbulence in fluvial boundary layers. *Geomorphology* 68 (1–2), 77–94.
- Byrd, T.C., Furbish, D.J., Warburton, J., 2000. Estimating depth-averaged velocities in rough channels. *Earth Surface Processes and Landforms* 25 (2), 167–173.
- Chartrand, S.M., Whiting, P.J., 2000. Alluvial architecture in headwater streams with special emphasis on step-pool topography. *Earth Surface Processes and Landforms* 25 (6), 583–600.
- Chin, A., 1999. The morphologic structure of step-pools in mountain streams. *Geomorphology* 27 (3–4), 191–204.
- Chin, A., 2003. The geomorphic significance of step-pools in mountain streams. *Geomorphology* 55 (1–4), 125–137.
- Chin, A., Wohl, E., 2005. Toward a theory for step pools in stream channels. *Progress in Physical Geography* 29 (3), 275–296.
- Clifford, N.J., French, J.R., 1993. Monitoring and modelling turbulent flow: historical and contemporary perspectives. In: Clifford, N.J., French, J.R., Hardisty, J. (Eds.), *Turbulence: Perspectives on Flow and Sediment Transport*. InWiley, Chichester, pp. 1–34.
- Comiti, F., 2003. Local scouring in natural and artificial step pool systems. PhD Thesis, University of Padua, Padua, 209 pp.
- Comiti, F., Andreoli, A., Lenzi, M.A., 2005. Morphological effects of local scouring in step-pool streams. *Earth Surface Processes and Landforms* 30 (12), 1567–1581.
- Curran, J.C., Wilcock, P.R., 2005. Characteristic dimensions of the step-pool bed configuration: An experimental study. *Water Resources Research* 41 (2), W02030. doi:10.1029/2004WR003568.
- Curran, J.H., Wohl, E.E., 2003. Large woody debris and flow resistance in step-pool channels, Cascade Range, Washington. *Geomorphology* 51 (1–3), 141–157.
- Daniels, M.D., Rhoads, B.L., 2003. Influence of a large woody debris obstruction on three-dimensional flow structure in a meander bend. *Geomorphology* 51 (1–3), 159–173.
- Elgar, S., Raubenheimer, B., Guza, R.T., 2001. Current meter performance in the surf zone. *Journal of Atmospheric and Oceanic Technology* 18 (10), 1735–1746.

- Faustini, J.M., Jones, J.A., 2003. Influence of large woody debris on channel morphology and dynamics in steep, boulder-rich mountain streams, western Cascades, Oregon. *Geomorphology* 51 (1–3), 187–205.
- Frizell, K.W., 2000. Effects of aeration on the performance of an ADV. In: Hotchkiss, R.H., Glade, M. (Eds.), *Water Resources 2000, Building Partnerships, Joint Conference on Water Resources Engineering and Water Resources Planning and Management*. ASCE, Minneapolis, MN.
- Frizell, K.H., Ehler, D.G., Mefford, B.W., 1994. Developing air concentration and velocity probes for measuring highly aerated, high-velocity flow. In: Pugh, C.A. (Ed.), *Fundamentals and Advancements in Hydraulic Measurements and Experimentation*. ASCE, Buffalo, NY, pp. 268–277.
- Furbish, D.J., 1993. Flow structure in a bouldery mountain stream with complex bed topography. *Water Resources Research* 29 (7), 2249–2263.
- Furbish, D.J., 1998. Irregular bed forms in steep, rough channels—I. Stability analysis. *Water Resources Research* 34 (12), 3635–3648.
- Grant, G.E., 1997. Critical flow constrains flow hydraulics in mobile-bed streams: A new hypothesis. *Water Resources Research* 33 (2), 349–358.
- Grant, G.E., Swanson, F.J., Wolman, M.G., 1990. Pattern and origin of stepped-bed morphology in high-gradient streams, western Cascades, Oregon. *Geological Society of America Bulletin* 102 (3), 340–352.
- Huhta, C., 2003. Personal communication. SonTek, Fort Collins, CO.
- Jackson, C.R., Sturm, C.A., 2002. Woody debris and channel morphology in first- and second-order forested channels in Washington's coast ranges. *Water Resources Research* 38 (9), 1177. doi:10.1029/2001WR001138.
- Keller, E.A., Melhorn, W.N., 1978. Rhythmic spacing and origin of pools and riffles. *Geological Society of America Bulletin* 89 (5), 723–730.
- Kostaschuk, R., Best, J., Villard, P., Peakall, J., Franklin, M., 2005. Measuring flow velocity and sediment transport with an acoustic Doppler current profiler. *Geomorphology* 68 (1–2), 25–37.
- Lamarre, H., Roy, A.G., 2005. Reach scale variability of turbulent flow characteristics in a gravel-bed river. *Geomorphology* 68 (1–2), 95–113.
- Lane, S.N., Biron, P.M., Bradbrook, K.F., Butler, J.B., Chandler, J.H., Crowell, M.D., McLelland, S.J., Richards, K.S., Roy, A.G., 1998. Three-dimensional measurement of river channel flow processes using acoustic Doppler velocimetry. *Earth Surface Processes and Landforms* 23 (13), 1247–1267.
- Lapointe, M., 1992. Burst-like sediment suspension events in a sand bed river. *Earth Surface Processes and Landforms* 17 (3), 253–270.
- Lee, A.J., Ferguson, R.I., 2002. Velocity and flow resistance in step-pool streams. *Geomorphology* 46 (1–2), 59–71.
- Legleiter, C.J., Phelps, T.L., Wohl, E.E., 2007. Geostatistical analysis of the effects of stage and roughness on reach-scale spatial patterns of velocity and turbulence intensity. *Geomorphology* 83, 322–345.
- MacFarlane, W.A., Wohl, E., 2003. Influence of step composition on step geometry and flow resistance in step-pool streams of the Washington Cascades. *Water Resources Research* 39 (2), 1037. doi:10.1029/2001WR001238.
- Matos, J., Frizell, K.H., Andre, S., Frizell, K.W., 2002. On the performance of velocity measurement techniques in air-water flows. In: Wahl, T.L., Pugh, C.A., Oberg, K.A., Vermeulen, T.B. (Eds.), *Hydraulic Measurements and Experimental Methods Conference 2002*. ASCE, Estes Park, CO.
- McLelland, S.J., Nicholas, A.P., 2000. A new method for evaluating errors in high-frequency ADV measurements. *Hydrological Processes* 14 (2), 351–366.
- Middleton, G.V., Southard, J.B., 1984. *Mechanics of Sediment Movement*, Lecture notes for S.E.P.M Short Course No. 3, 2nd ed. Providence, RI.
- Middleton, G.V., Wilcock, P.R., 1994. *Mechanics in the Earth and Environmental Sciences*. Cambridge University Press, Cambridge.
- Milzow, C., Molnar, P., McArdell, B.W., Burlando, P., 2006. Spatial organization in the step-pool structure of a steep mountain stream (Vogelbach, Switzerland). *Water Resources Research* 42, W04418. doi:10.1029/2004WR003870.
- Nelson, J.M., Shreve, R.L., McLean, S.R., Drake, T.G., 1995. Role of near-bed turbulence structure in bed-load transport and bed form mechanics. *Water Resources Research* 31 (8), 2071–2086.
- Nezu, I., Nakagawa, H., 1993. *Turbulence in Open-Channel Flows*. IAHR Monograph Series. A.A. Balkema, Rotterdam. 281 pp.
- Nikora, V.I., Goring, D.G., 1998. ADV measurements of turbulence: Can we improve their interpretation? *Journal of Hydraulic Engineering* 124 (6), 630–634.
- Peterson, D.F., Mohanty, P.K., 1960. Flume studies of flow in steep, rough channels. *Journal of the Hydraulics Division-ASCE* 86 (HY9), 55–76.
- Robert, A., 1993. Bed configuration and microscale processes in alluvial channels. *Progress in Physical Geography* 17 (2), 123–136.
- Robert, A., Roy, A.G., De Serres, B., 1992. Changes in velocity profiles at roughness transitions in coarse-grained channels. *Sedimentology* 39 (5), 725–735.
- Robert, A., Roy, A.G., De Serres, B., 1996. Turbulence at a roughness transition in a depth limited flow over a gravel bed. *Geomorphology* 16 (2), 175–187.
- Roy, A.G., Biron, P., De Serres, B., 1996. On the necessity of applying a rotation to instantaneous velocity measurements in river flows. *Earth Surface Processes and Landforms* 21 (9), 817–827.
- Roy, A.G., Buffin-Belanger, T., Lamarre, H., Kirkbride, A.D., 2004. Size, shape and dynamics of large-scale turbulent flow structures in a gravel-bed river. *Journal of Fluid Mechanics* 500, 1–27.
- SAS, 2004. *Statistical Analysis Software*, Cary, NC.
- SonTek, 2001. *FlowTracker Handheld ADV Technical Documentation*, San Diego, CA.
- SonTek/YSI, 2001. *Acoustic Doppler Velocimeter Principles of Operation*, San Diego, CA.
- Sukhodolov, A., Thiele, M., Bungartz, H., 1998. Turbulence structure in a river reach with sand bed. *Water Resources Research* 34 (5), 1317–1334.
- Sukhodolov, A.N., Rhoads, B.L., 2001. Field investigation of three-dimensional flow structure at stream confluences 2. Turbulence. *Water Resources Research* 37 (9), 2411–2424.
- USGS, 1977. *National Handbook of Recommended Methods for Water-Data Acquisition*. U.S. Geological Survey, Reston, VA.
- Valle, B.L., Pasternack, G.B., 2002. TDR measurements of hydraulic jump aeration in the South Fork of the American River, California. *Geomorphology* 42 (1–2), 153–165.
- Valle, B.L., Pasternack, G.B., 2006. Field mapping and digital elevation modelling of submerged and unsubmerged hydraulic jump regions in a bedrock step-pool channel. *Earth Surface Processes and Landforms* 31 (6), 646–664.
- Valle, B.L., Pasternack, G.B., in press. Air concentrations of submerged and unsubmerged hydraulic jumps in a bedrock step-pool channel. *Journal of Geophysical Research-Earth Surface*.



- Voulgaris, G., Trowbridge, J.H., 1998. Evaluation of the acoustic Doppler velocimeter (ADV) for turbulence measurements. *Journal of Atmospheric and Oceanic Technology* 15 (1), 272–289.
- Wahl, T.L., 2000. Analyzing ADV data using WinADV. In: Hotchkiss, R.H., Glade, M. (Eds.), *Water Resources 2000, Building Partnerships, Joint Conference on Water Resources Engineering and Water Resources Planning and Management*. ASCE, Minneapolis, MN.
- Walker, I.J., Roy, A.G., 2005. Fluid flow and sediment transport processes in geomorphology: innovations, insights, and advances in measurement. *Geomorphology* 68 (1–2), 1–2.
- Whittaker, J.G., Jaeggi, M.N.R., 1982. Origin of step-pool systems in mountain streams. *Journal of the Hydraulics Division-ASCE* 108 (6), 758–773.
- Wilcox, A.C., 2005. Interactions between hydraulics and morphology in step-pool stream channels. PhD Thesis, Colorado State University, Fort Collins, CO.
- Wilcox, A.C., Wohl, E.E., 2006. Flow resistance dynamics in step-pool channels: 1. Large woody debris and controls on total resistance. *Water Resources Research* 42, W05418. doi:10.1029/2005WR004277.
- Wilcox, A.C., Nelson, J.M., Wohl, E.E., 2006. Flow resistance dynamics in step-pool channels: 2. Partitioning between grain, spill, and woody debris resistance. *Water Resources Research* 42, W05419. doi:10.1029/2005WR004278.
- Wohl, E.E., Grodek, T., 1994. Channel bed-steps along Nahal-Yael, Negev Desert, Israel. *Geomorphology* 9 (2), 117–126.
- Wohl, E.E., Thompson, D.M., 2000. Velocity characteristics along a small step-pool channel. *Earth Surface Processes and Landforms* 25 (4), 353–367.
- Yager, E., Kirchner, J.W., Dietrich, W.E., Furbish, D.J., 2002. Prediction of sediment transport in steep boulder-bed channels. *EOS Trans. AGU Fall Meet. Suppl.* 83 (47) Abstract H21G-03.
- Zimmerman, A., Church, M., 2001. Channel morphology, gradient profiles and bed stresses during flood in a step-pool channel. *Geomorphology* 40 (3–4), 311–327.